BMC Microbiology

RESEARCH

Open Access

Contribution of *fepA*$_{sm}$, *fciABC*, *sbaA*, *sbaBCDEF*, and *feoB* to ferri-stenobactin acquisition in *Stenotrophomonas maltophilia* KJ

Ting-Yu Yeh[1†], Hsu-Feng Lu[2†], Li-Hua Li[3,4], Yi-Tsung Lin[5,6] and Tsuey-Ching Yang[1*]

Abstract

Background *Stenotrophomonas maltophilia,* an opportunistic pathogen, is ubiquitously distributed in the environment. In response to iron-depletion stress, *S. maltophilia* synthesizes the sole catecholate-type siderophore, stenobactin, for ferric iron acquisition. FepAsm, a TonB-dependent transporter (TBDT), is the sole known outer membrane receptor responsible for ferri-stenobactin uptake in *S. maltophilia* K279a. However, *S. maltophilia* KJ and its isogenic *fepA* mutant displayed comparable ability to utilize $FeCl_3$ as the sole iron source for growth in iron-depleted conditions, suggesting the involvement of additional TBDT in ferri-stenobactin uptake in the KJ strain. Here, we aimed to determine additional TBDT required for ferri-stenobactin uptake and the post-TBDT ferri-stenobactin transport system in the KJ strain.

Methods and results Twelve TBDTs, whose expression were significantly upregulated in 2,2'-dipyridyl-treated KJ strain, were selected as candidates for ferri-stenobactin uptake. The involvement of these selected candidates in ferri-stenobactin acquisition was investigated using deletion mutant construction and $FeCl_3$ utilization assay. Among the 12 TBDTs tested, FepAsm, FciA, and SbaA were the TBDTs for ferri-stenobactin uptake in KJ strain. Because *fciA* is a member of *fciTABC* operon, the involvement of *fciTABC* operon in ferri-stenobactin uptake was also investigated. Of the *fciTABC* operon, *fciA, fciB* and *fciC*, but not *fciT*, contributed to ferri-stenobatin acquisition. SbaE is the homolog of FepD/FepG, the inner membrane transporters for ferri-enterobactin in *E. coli*; therefore, *sbaBCDEF* operon was selected as a candidate for the post-TBDT transport system of ferri-stenobactin. All proteins encoded by *sbaBCDEF* operon participated in ferri-stenobactin acquisition. Due to the contribution of the putative periplasmic esterase SbaB to ferri-stenobactin acquisition, FeoB, a ferrous iron inner membrane transporter, was included as a candidate and proved to be involved in ferri-stenobactin acquisition. Accordingly, contributions of *feoB* and *sbaE* to ferri-stenobactin acquisition illustrated that ferric and ferrous iron could be transported across the inner membrane via SbaE and FeoB, respectively.

Conclusions *FepAsm*, *fciABC*, *sbaA*, *sbaBCDEF*, and *feoB* contribute to ferri-stenobatin acquisition in *Stenotrophomonas maltophilia* KJ.

Keywords *Stenotrophomonas*, Siderophore, Iron acquisition, Virulence, TonB-dependent transporter

†Ting-Yu Yeh and Hsu-Feng Lu contributed equally to this work.

*Correspondence:
Tsuey-Ching Yang
tcyang@nycu.edu.tw
Full list of author information is available at the end of the article

Background

Iron, an essential element for bacterial pathogens, plays a significant role in signaling pathways and is used as a cofactor or prosthetic group for several proteins required for growth and development [1, 2]. Ferric iron has low solubility under biological pH and aerobic conditions [3]; thus, it is sequestered by biomolecules in the human serum, making it inaccessible to pathogens [4]. To survive in the host, pathogens have evolved several mechanisms for iron acquisition. First, pathogens can utilize specific TonB-dependent transporters (TBDTs) to directly acquire iron from sequestered sources, such as hemin, ferritin, and transferrin. Second, pathogens can synthesize and secrete iron chelators such as siderophores, hemophores, and citrate to acquire iron [2]. These iron-containing complexes are specifically uptaken by their cognate TBDTs and are subsequently transported to the periplasm and cytosol for utilization [5].

Siderophores have a high affinity for ferric iron. Secreted siderophores bind to ferric iron to form a ferri-siderophore complex; however, the capability of siderophores to form stable complexes with ferrous iron is low. Based on the structure of their chelate-forming sites, siderophores can be classified as hydroxamates, catecholates, carboxylates, phenolates, and mixed types [6]. Enterobactin of *Escherichia coli* is the best well-known catecholate-type siderophore. Under iron-depletion stress, enterobactin is synthesized in a non-ribosomal peptide synthetase (NRPSs)-dependent manner [4] via the action of EntA, EntB, EntC, EntD, EntE, and EntF enzymes. The synthesized enterobactins are secreted into the periplasm via the inner membrane protein EntS and then exported into the extracellular environment via tripartite efflux pumps [7]. Enterobactin captures ferric iron and the resultant ferri-enterobactin is mainly uptaken by TBDT FepA [8]. Once across the outer membrane, ferri-enterobactin is shuttled by the periplasmic enterobactin-binding protein FepB and delivered to the cytoplasmic transmembrane transporters FepD and FepG. The transport of ferri-enterobactin across the cytoplasmic membrane is an ATP-dependent process that is mediated by the ATP-binding protein FepC [4]. In the cytoplasm, enterobactin is hydrolyzed by esterase Fes, releasing ferric iron [9]. Alternatively, ferric iron in enterobactin is reduced by the NADPH-dependent reductase YqjH, which releases ferrous iron [10].

The expression of genes associated with siderophore synthesis, secretion, uptake, release, and energy supply is tightly regulated by pathogens. In bacteria, iron homeostasis is modulated at the transcriptional level by the ferric uptake repressor Fur. When an adequate concentration of iron is present, Fur functions as a repressor [11, 12]. The Fur-Fe^{2+} complex binds to consensus DNA sequences, termed Fur boxes, located in the promoter region of these Fur-regulated genes and represses gene expression [13]. Iron depletion serves as a signal to release the Fur protein from the Fur box and trigger the expression of Fur regulon genes.

Stenotrophomonas maltophilia is ubiquitously distributed in the environment and regarded as an opportunistic pathogen [14]. *S. maltophilia* infections are difficult to treat due to its intrinsic and acquired resistance to several antibiotics such as aminoglycosides, β-lactams, and macrolides [15]. Iron homeostasis is crucial for pathogens; hence, a comprehensive understanding of iron homeostasis may provide new insights into the control of pathogenic infections [16].

Given its diverse habitats, *S. maltophilia* has evolved many iron-acquisition systems [17]. The characterized iron acquisition systems of *S. maltophilia* include the PacIRA system for *Pseudomonas aeruginosa* pyrochelin [18], the FciTABC-FeoABI system for ferric citrate uptake [19], the HemA-HemU-TonB1 system for hemin uptake in the KJ strain [20, 21], and FepA TBDT for ferri-siderophore uptake in the K279a strain [22]. In response to iron-depletion stress, *S. maltophilia* can synthesize a catecholate-type siderophore, stenobactin, relying on *entCEBB'FA* gene cluster [23]. SmeYZ, SmeDEF, and SbiAB pumps are known outlets for stenobactin export [24]. Once bound to ferric iron, ferri-stenobactin is uptaken by TBDT FepA [25]. Nas and Cianciotto demonstrated that FepA appears to be the sole TBDT for ferri-stenobactin uptake in the K279a strain, because its *fepA* deletion mutant cannot utilize ferri-stenobactin as an iron source for growth in iron-depleted conditions [22]. Excep for FepA, little is known about how ferri-stenobactin is acquired for utilization. In our recent study, we noticed that the *fepA* deletion mutant of KJ strain, a clinical isolate isolated in Taiwan, displayed comparable viability with wild-type KJ in 2,2′-dipyridyl (DIP)- and $FeCl_3$-supplemented medium (Fig. 1), suggesting that the involvement of additional TBDT for ferri-stenobactin uptake is not yet fully elucidated. In this study, we sought to identify additional TBDTs involved in ferri-stenobactin uptake in the KJ strain. In addition, a post-outer-membrane transport system for ferri-stenobactin acquisition was also investigated.

Methods

Bacterial strains, plasmids, and primers

The bacterial strains and plasmids used in this study were summarized in Table S1. Table S2 lists the sequences and purposes of the primers used in this study.

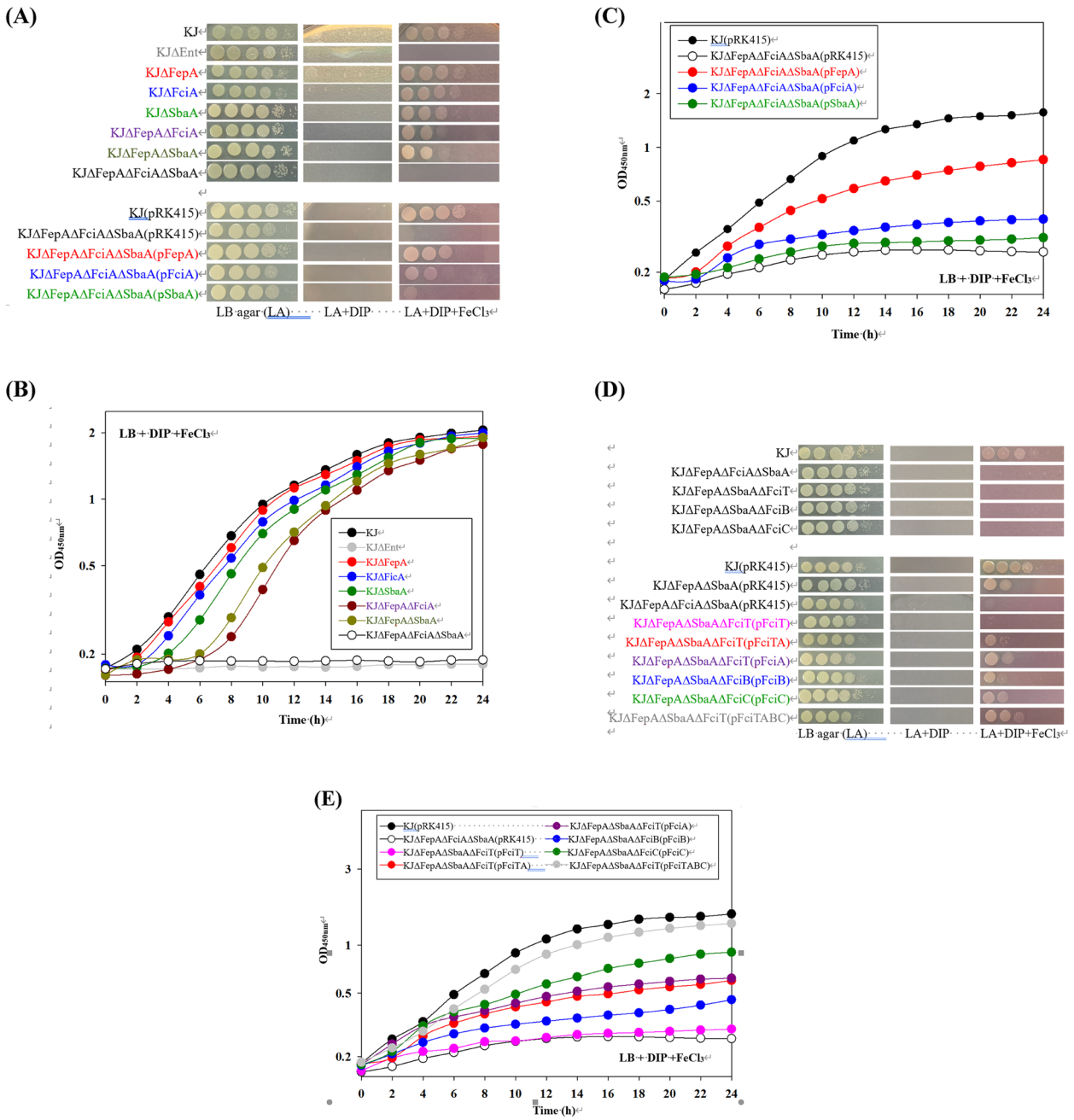

Fig. 1 Roles of *fepA*, *sbaA*, and *fciTABC* in ferri-stenobactin acquisition in iron-depleted conditions. For cell viability, the logarithmic-phase bacterial cells tested of 2×10^5 CFU/μL were tenfold serially diluted. A bacterial aliquot (5 μL) was spotted on the LB agar plates as indicated. After a 24-h incubation at 37℃, bacterial viability was imaged. For growth curve, overnight culture was inoculated into LB broth with DIP and $FeCl_3$ at an initial OD_{450nm} of 0.15. Bacterial growth was monitored for 24 h. The concentrations of 2,2′-dipyridyl (DIP) and $FeCl_3$ used were 50 μg/mL and 35 μM, respectively. The images and graphs are representatives of at least three replicated experiments. **A** Cell viability of wild-type KJ and its derived *fepA*-, *fciA*-, and *sbaA*-associated mutants in DIP and $FeCl_3$-supplemented LB agar. **B** Growth curve of wild-type KJ and its derived *fepA*-, *fciA*-, and *sbaA*-associated mutants in DIP and $FeCl_3$-supplemented LB broth. **C** Growth curve of wild-type KJ, KJΔFepAΔFciAΔSbaA, and KJΔFepAΔFciAΔSbaA-derived complementary strains in DIP and $FeCl_3$-supplemented LB broth. **D** Cell viability of wild-type KJ and its derived *fepA*-, *fciTABC*-, and *sbaA*-associated mutants in DIP and $FeCl_3$-supplemented LB agar. **E** Growth curve of wild-type KJ and *fciTABC* operon-associated complementary strains in DIP and $FeCl_3$-supplemented LB broth

Construction of in-frame deletion mutants

A double-crossover recombination strategy was used to construct in-frame deletion mutants, as described previously [26]. Briefly, two DNA fragments containing the upstream and downstream regions of the intended deletion region were amplified by PCR from *S. maltophilia* KJ and subsequently cloned into pEX18Tc to generate pEX18Tc-derived recombinant plasmids (Table S1). Table S2 lists the primers used. The pEX18Tc-derived recombinant plasmids were transferred to *S. maltophilia* KJ via conjugation. Transconjugant selection and double-crossover mutant confirmation were performed as described previously [26].

Construction of complementation plasmids

The target gene for the complementation assay was amplified by PCR and subsequently cloned into pRK415. The resulting plasmids were transferred into the assayed strains via conjugation. Primers used to construct the complementary plasmids were listed in Table S2.

Iron source utilization assay-cell viability

An iron source utilization assay was conducted to assess the ability of the bacteria to utilize exogenous iron sources under iron-depleted conditions. The addition of 50 μg/mL DIP was enough to create an iron-limited condition, in which KJ cells lost viability unless an exogenous iron source was supplied [23]. The logarithmic-phase cells of 2×10^5 CFU/μL were tenfold serially diluted. Five microliters of bacteria were spotted onto agar plates, as indicated. After a 24-h incubation at 37℃, bacterial growth was observed and recorded. Each experiment was conducted in triplicate.

Iron source utilization assay-growth curve

Overnight culture was inoculated into LB broth with DIP (50 μg/mL) and $FeCl_3$ (35 μM) at an initial OD_{450nm} of 0.15. Bacterial growth was monitored by recording the OD_{450nm} of bacterial aliquot at an interval of 2 h. Each experiment was conducted in triplicate.

Reverse-transcription PCR and operon verification

DNA-free RNA was isolated from KJ cells treated with 30 μg/mL DIP. Reverse transcription was conducted using the SbaF-C primer. The SbaF-C-derived cDNA was used as the template for PCR with the primer sets SbaBQ94-F/R, SbaCQ106-F/R, SbaDQ98-F/R, SbaEQ92-F/R, SbaFQ108-F/R, and 2358Q86-F/R (Table S2). The PCR products were separated by 2% agarose gel electrophoresis and visualized by ethidium bromide staining.

Quantitative real-time PCR (qRT-PCR)

DNA-free RNA was prepared from mid-exponential phase bacterial cells and converted to cDNA using a High-Capacity cDNA Reverse Transcription Kit (Applied Biosystems). qRT-PCR was performed using the StepOnePlus Real-Time PCR System following the manufacturer's protocol. The primer sets used were listed in Table S2. Gene expression levels were normalized to those of 16S rRNA. Fold change was calculated using the $\Delta\Delta C_T$ method [27]. All experiments were performed at least three times.

Results

FepAsm is not the sole receptor for ferri-stenobactin uptake in KJ strain

In our previous study, we established an iron source utilization assay to evaluate bacterial iron utilization in iron-depleted conditions [23]. Consistent with our previous reports, the KJ strain lost viability in 50 μg/mL DIP-containing LB agar and reverted viability when 35 μM $FeCl_3$ was added to the media (Fig. 1A). However, KJΔEnt, a stenobactin-null isogenic mutant [23], was unable to restore growth in $FeCl_3$-containing medium (Fig. 1A), verifying that stenobactin-mediated iron acquisition is the dominant way to support bacterial growth in our assay system.

FepA is a critical TBDT for enterobactin uptake in *E. coli* [8]. The FepA homolog (Smlt1426) has been reported to be the sole TBDT responsible for ferri-stenobactin uptake in *S. maltophilia* K279a because the *fepA* deletion mutant of *S. maltophilia* K279a cannot utilize $FeCl_3$ as the sole iron source to support growth in iron-depleted conditions [22]. To distinguish Smlt1426 from *E. coli* FepA, we designated Smlt1426 as FepAsm. *S. maltophilia* KJ was used as the parental strain in our series of studies on iron utilization [18–21, 23, 24, 26, 28]. We noticed that the *fepAsm* deletion mutant of *S. maltophilia* KJ, KJΔFepA, displayed comparable viability in DIP- and $FeCl_3$-supplemented medium to wild-type KJ (Fig. 1A), indicating that FepAsm is not the sole receptor for ferri-stenobactin uptake in the KJ strain.

FepAsm, FciA, and SbaA are the receptors for ferri-stenobactin uptake in KJ strain

Two approaches were used to select TBDT candidates for ferri-stenobactin uptake. First, the *S. maltophilia* K279a genome was queried for homologs of known iron-acquisition TBDTs from other bacteria. Second, it is presumed that iron acquisition systems are upregulated in iron-depleted conditions. The comparative transcriptome

analysis of wild-type KJ with and without DIP treatment was available in our recent study [24]. By integrating the homolog prediction and transcriptome data, we identified 12 candidates, whose expression are significantly upregulated in DIP-treated condition (at least tenfold upregulation compared to non-treated counterpart), including *hemA* (Smlt0795), *fciA* (Smlt1148), Smlt1233, *fepAsm* (Smlt1426), Smlt1762, *pacA* (Smlt2666), Smlt2714, *fecA* (Smlt2858), Smlt2937, Smlt3022, Smlt3898, and Smlt4135 (designated as SbaA, stenobactin receptor, based on the following study) (Table S3).

To determine their involvement in ferri-siderophore uptake, we constructed 12 TBDT deletion mutants in KJ to test their ability to utilize $FeCl_3$ as the sole iron source to support growth in iron-depleted conditions. In the following study, cell viability and growth curve assays were used to assess bacterial ability to utilize $FeCl_3$ as the sole iron source to support growth in solid and liquid media, respectively. All tested mutants exhibited noticeable cell viability in DIP- and $FeCl_3$-supplemented LB agar (KJΔFepA, KJΔFciA, and KJΔSbaA as representatives in Fig. 1A), and broth (KJΔFepA, KJΔFciA, and KJΔSbaA as representatives in Fig. 1B), suggesting that the 12 TBDTs were not individually critical for ferri-stenobactin uptake in *S. maltophilia*.

Considering the possibility of functional redundancy in TBDTs, we constructed double mutants of TonB-dependent receptors using KJΔFepA as the parental strain, which yielded KJΔFepAΔHemA, KJΔFepAΔFciA, KJΔFepAΔ1233, KJΔFepAΔ1762, KJΔFepAΔPacA, KJΔFepAΔ2714, KJΔFepAΔ2858, KJΔFepAΔ2937, KJΔFepA3022, KJΔFepAΔ3898, and KJΔFepAΔSbaA. Of the 11 double mutants tested, KJΔFepAΔFciA and KJΔFepAΔSbaA displayed compromised viability in DIP- and $FeCl_3$-supplemented LB agar (Fig. 1A) and broth (Fig. 1B). A *fepAsm*, *fciA*, and *sbaA* triple mutant, KJΔFepAΔFciAΔSbaA, was constructed. No viability was observed when KJΔFepAΔFciAΔSbaA grew in DIP- and $FeCl_3$-containing LB agar (Fig. 1A) and broth (Fig. 1B). Complementation of KJΔFepAΔFciAΔSbaA with *fepAsm*-, *fciA*-, and *sbaA*-containing plasmids, respectively, partially restored the viability in the DIP- and $FeCl_3$-supplemented LB agar (Fig. 1A) and broth (Fig. 1C), verifying the contribution of FepAsm, FciA, and SbaA to the ferri-stenobactin uptake.

FciA, FciB, and FciC contribute to ferri-stenobactin acquisition in KJ strain

Since *fciA* is a member of the *fciTABC* operon [19], we were interested in understanding the involvement of *fciT*, *fciB*, and *fciC* in ferri-stenobactin acquisition. Introduction of *ΔfciT*, *ΔfciB*, and *ΔfciC* alleles into the chromosome of KJΔFepAΔSbaA respectively resulted in a loss of cell viability in DIP- and $FeCl_3$-supplemented LB agar (Fig. 1D), and individual complementary strains, except *fciT*, partially restored viability (Fig. 1D and E). It is known that the inactivation of *fciT* has a polar effect on the expression of *fciA,* but not on *fciB* and *fciC* [19]. To further clarify *fciT* involvement in ferri-stenobactin acquisition, KJΔFepAΔSbaAΔFciT was complemented with *fciA* and *fciT-fciA* genes, respectively, and the resultant complementary strains were subjected to a $FeCl_3$ utilization assay. KJΔFepAΔSbaAΔFciT complemented with *fciA* and *fciT-fciA* displayed comparable ability in $FeCl_3$ utilization (Fig. 1D and E), ruling out the contribution of *fciT* to ferri-stenobactin acquisition. Collectively, FciA, FciB, and FciC are involved in ferri-stenobactin acquisition.

Smlt2353-2357 (*sbaBCDEF*) operon contribute to ferri-stenobactin acquisition in KJ strain

To consider the post-TBDT transport system of ferri-stenobactin, the FepB-FepD/FepG-FepC-Fes-YqjH system of *E. coli* is the closest model for reference. A genome-wide survey of *S. maltophilia* K279a, using FepD and FepG as query, revealed that Smlt2356 was the candidate. Smlt2356 (designated as SbaE hereafter) encodes an inner membrane protein that displayed 35%/50% and 31%/51% identity/similarity with FepD and FepG proteins of *E. coli*, respectively. Surrounding *sbaE*, a five-gene cluster (Smlt2353-Smlt2357), which resembles an operon encoding a putative iron-complex transportation system, attracted our attention because it was co-upregulated in DIP-treated KJ cells (Table S3) [24]. These genes (named *sbaBCDEF*) encode a putative periplasmic esterase SbaB, a periplasmic ATP-binding protein SbaC, a periplasmic ABC transporter substrate-binding protein SbaD, an inner membrane ABC transporter permease SbaE, and a cytosolic ABC transporter ATP-binding protein SbaF (Fig. 2A). To assess whether the *sbaBCDEF* genes were organized into an operon, RT-PCR was performed, and the results indicated the presence of a *sbaBCDEF* transcript (Fig. 2B).

To investigate the involvement of *sbaBCDEF* operon in ferri-stenobactin acquisition, an in-frame deletion mutant of each gene was constructed, generating KJΔSbaB, KJΔSbaC, KJΔSbaD, KJΔSbaE, and KJΔSbaF. These mutants and their complementary strains were subjected to cell viability assay and growth curve assay. Compared to wild-type KJ, all mutants tested displayed compromised viability in DIP- and $FeCl_3$-supplemented LB agar (Fig. 2C) and poor growth in DIP- and $FeCl_3$-supplemented LB broth (Fig. 2D). Individual complementary strains, except *sbaE*, restored their ability to utilize $FeCl_3$ as the sole iron source (Fig. 2C and E). Failure of *sbaE* complementation led us to consider the polar

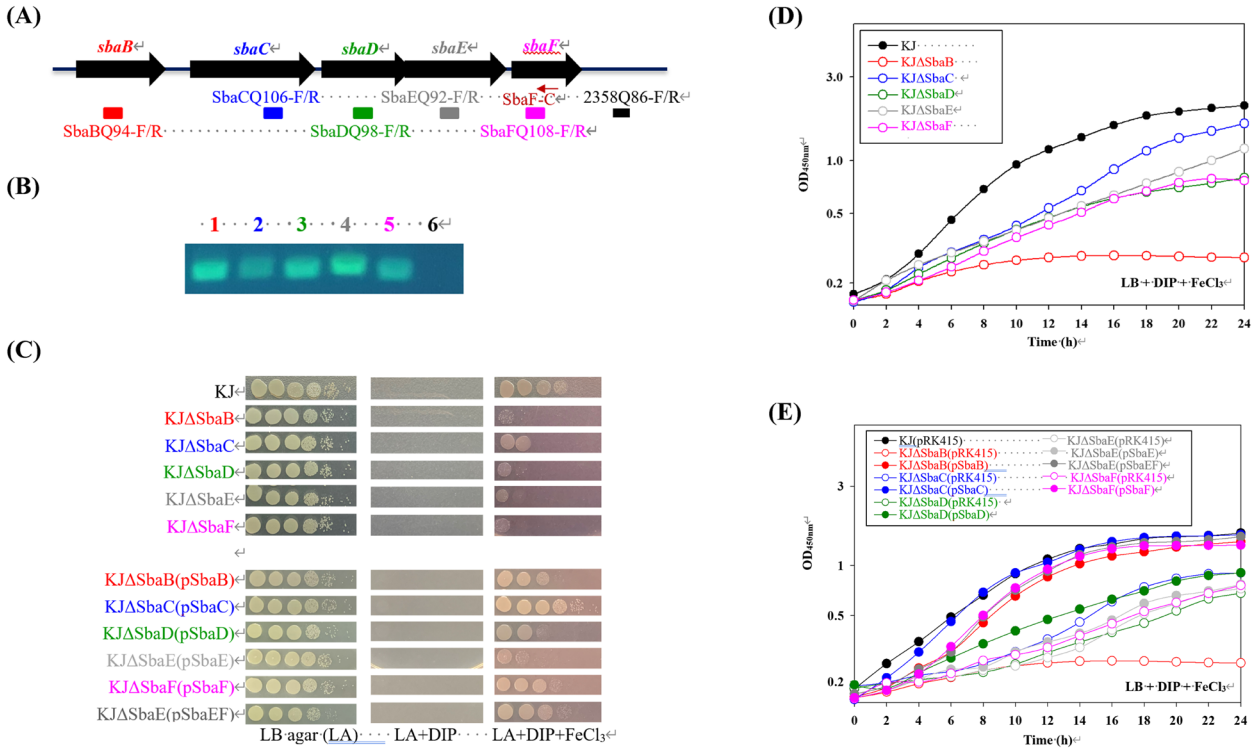

Fig. 2 *sbaBCDEF* is an operon and contributes to ferri-stenobactin acquisition in iron-depleted conditions. **A** The genetic organization of *sbaBCDEF* operon in *S. maltophilia*. Black arrows represent genes and the direction of transcription. The small red arrow indicates the position of primer SbaF-C used for reverse transcription. Bars represent the positions of PCR amplicons amplified using the primer pairs labeled above or below the bars. **B** Agarose gel electrophoresis of the PCR products. DNA-free RNA was prepared from KJ cells treated with 30 μg/mL DIP and cDNAs were obtained by reverse transcription using primer SbaF-C. The cDNA was used as the template for PCR. PCR amplicons were separated by 2% agarose gel electrophoresis and stained with ethidium bromide. Lane 1, PCR amplicon generated by SbaBQ94-F and SbaBQ94-R; lane 2, PCR amplicon generated by SbaCQ106-F and SbaCQ106-R; lane 3, PCR amplicon generated by SbaDQ98-F and SbaDQ98-R; lane 4, PCR amplicon generated by SbaEQ92-F and SbaEQ92-R; lane 5, PCR amplicon generated by SbaFQ108-F and SbaFQ108-R; lane 6, PCR amplicon generated by 2358Q86-F and 2358Q86-R. The 2358Q86-F/R primer pairs were used as a control for a check of DNA contamination during cDNA preparation. **C** Cell viability of wild-type KJ and its derived *sbaBCDEF*-associated mutants in DIP and $FeCl_3$-supplemented LB agar. The logarithmic-phase bacterial cells tested of 2×10^5 CFU/μL were tenfold serially diluted. A bacterial aliquot (5 μL) was spotted on the LB agar plates as indicated. After a 24-h incubation at 37℃, bacterial viability was imaged. The image is a representative of at least three replicated experiments. **D** Growth curve of wild-type KJ and its derived *sbaBCDEF*-associated mutants in DIP and $FeCl_3$-supplemented LB broth. Overnight culture was inoculated into LB broth with DIP and $FeCl_3$ at an initial OD_{450} of 0.15. Bacterial growth was monitored for 24 h. The concentrations of 2,2′-dipyridyl (DIP) and $FeCl_3$ used were 50 μg/mL and 35 μM, respectively. The graph is a representative of at least three replicated experiments. **E** Growth curve of wild-type KJ and its derived *sbaBCDEF*-associated complementary strains in DIP and $FeCl_3$-supplemented LB broth. Overnight culture was inoculated into LB broth with DIP and $FeCl_3$ at an initial OD_{450nm} of 0.15. Bacterial growth was monitored for 24 h. The concentrations of DIP and $FeCl_3$ used were 50 μg/mL and 35 μM, respectively. The graph is a representative of at least three replicated experiments

effect of *sbaE* deletion on *sbaF* expression. The presence of a polar effect was verified using qRT-PCR (data not shown). Complementation of KJΔSbaE with pSbaEF, a plasmid containing *sbaE* and *sbaF* genes, restored the viability in the DIP- and $FeCl_3$-supplemented media (Fig. 2C and E). Thus, *sbaBCDEF* operon participates in post-TBDT transportation of ferri-stenobactin.

FeoB contribute to ferri-stenobactin acquisition in KJ strain

SbaB is annotated as a periplasmic esterase and the above results demonstrated its contribution to ferri-stenobactin acquisition (Fig. 2C, D, and E). These observations suggested that ferri-stenobactin may be hydrolyzed by SbaB in the periplasm. If this is the case, we wonder whether the released ferric iron is reduced by reductase in the periplasm or is immediately transported into the cytoplasm. If the former occurs, the reduced ferrous iron might be transported into the cytoplasm via FeoB [19]. To test this hypothesis, the cell viability and growth curve of KJΔFeoB, a *feoB* deletion mutant [19], in DIP- and $FeCl_3$-containig medium was investigated. Compared to the wild-type KJ, KJΔFeoB displayed a compromised ability to grow in DIP- and $FeCl_3$-containing LB agar (Fig. 3A) and LB broth

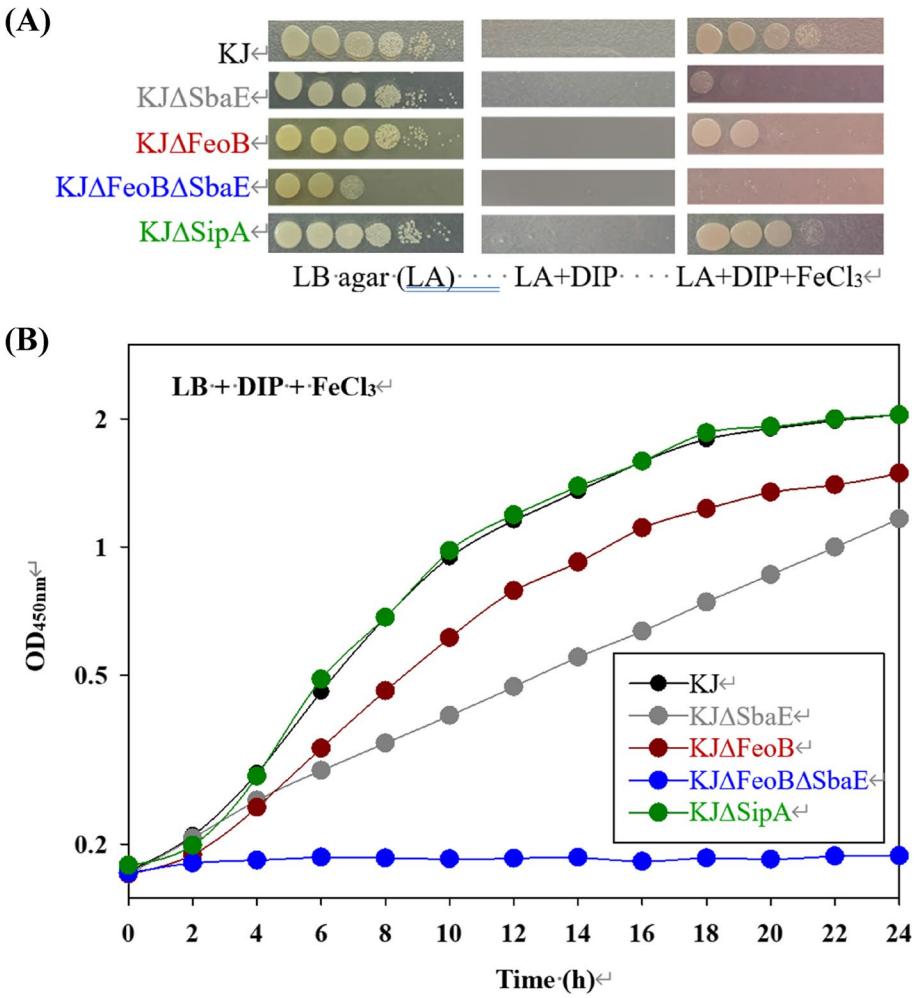

Fig. 3 Role of *sbaE*, *feoB*, and *sipA* in ferri-stenobactin acquisition in iron-depleted conditions. **A** The logarithmic-phase bacterial cells tested of 2×10^5 CFU/μL were tenfold serially diluted. A bacterial aliquot (5 μL) was spotted on the LB agar plates as indicated. After a 24-h incubation at 37℃, bacterial viability was imaged. The image is a representative of at least three replicated experiments. **B** Overnight culture was inoculated into LB broth with DIP and $FeCl_3$ at an initial OD_{450nm} of 0.15. Bacterial growth was monitored for 24 h. The concentrations of 2,2′-dipyridyl (DIP) and $FeCl_3$ used were 50 μg/mL and 35 μM, respectively. The graph is a representative of at least three replicated experiments

(Fig. 3B). Furthermore, we also observed that a *feoB* and *sbaE* double mutant, KJΔFeoBΔSbaE, lost viability in DIP- and $FeCl_3$-containing media (Fig. 3A & B).

SipA (Smlt3577), a YqjH homolog, is not involved in ferri-stenobactin utilization

In the *E. coli* model, iron detachment from ferri-enterobactin occurs in the cytoplasm via enterobactin esterase (Fes) and YqjH [9, 10]. *S. maltophilia* K279a genome survey was conducted to identify possible *fes* and *yqjH* homologs. Smlt3577, an *yqjH* homolog, was discovered; however, no significant hits for *fes* were observed. The protein encoded by Smlt3577 was annotated as a siderophore-interacting FAD-binding protein (designated as SipA hereafter), which showed 29% similarity and 41% identity with *E. coli* YqjH. To investigate the role of SipA in ferri-stenobactin acquisition, KJΔSipA was constructed and subjected to the $FeCl_3$ utilization assay. KJΔSipA and wild-type KJ showed comparable cell viability in DIP- and $FeCl_3$-containing LB agar (Fig. 3A) and broth (Fig. 3B), ruling out the involvement of SipA in ferri-stenobactin acquisition.

Ferri-stenobactin acquisition-associated genes are regulated by Fur and iron availability

Fur is a global regulator involved in iron homeostasis [29]. Thus, the role of Fur in the expression of *fepAsm*, *fciTABC* operon, *sbaA*, *sbaBCDEF* operon, and *feoABI*

operon was investigated using qRT-PCR. Compared to wild-type KJ, *fepAsm*, *fciA*, *sbaA*, and *sbaE* transcripts were increased in *fur* mutant and almost reverted to wild-type level when *fur* was complemented. Furthermore, DIP treatment-mediated iron limitation also upregulated the expression of *fepAsm*, *fciA*, *sbaA*, and *sbaE*. However, *feoB* transcript level was hardly affected by *fur* inactivation and DIP treatment (Fig. 4). Therefore, the ferri-stenobactin acquisition-associated genes, except *feoB*, are regulated by Fur and iron availability.

Discussion

As a highly conserved iron assimilation pathway in gram-negative bacteria, ferri-siderophore acquisition requires the coordination of multiple components from the outer membranes to the cytoplasm. Stenobactin is the only catecholate-type siderophore in *S. maltophilia*. Enterobactin of *E. coli* is a well-characterized catecholate-type siderophore. The homologs of *E. coli* enterobactin synthesis genes are highly conserved in *S. maltophilia* genome, except *entD* [30], highly suggesting that the acquisition systems for ferri-enterobactin and ferri-stenobactin share some degree of similarity. Nas and Cianciotto have demonstrated that the *fepA* mutant of *S. maltophilia* K279a is unable to utilize ferric iron as the sole iron source to support growth in iron-depleted conditions [22], indicating that FepAsm is the sole (or primary) TBDT for stenobactin uptake. There are at least five known TBDTs capable of ferri-enterobactin uptake in *E. coli,* but the five TBDT genes are not highly conserved in all *E. coli* isolates [31]. Thus**,** the functional redundancy of TBDTs in bacterial species is common, but the types of redundant TBDTs may vary among different isolates. Our study is the first to demonstrate that FciA and SbaA function as ferri-stenobactin receptors in addition to FepAsm in *S. maltophilia* KJ (Fig. 1). We noticed that complementation of triple mutant KJΔFepAΔFciAΔSbaA with *sbaA* barely restored viability in DIP- and $FeCl_3$-supplemented media compared to complementation with *fepA* or *fciA*; however, KJΔFepAΔFciA still kept moderate viability in DIP- and $FeCl_3$-supplemented media (Fig. 1). This observation suggested that of the three TBDTs, SbaA seems to exhibit the poorest ability in ferri-stenobactin uptake. However, SbaA may be complementarily upregulated in the case of *fepAsm* and *fciA* inactivation.

Potential advantages of TBDT redundancy include (i) insurance against iron acquisition if one TBDT loses function, (ii) increased ability of a pathogenic strain to acquire iron during host infection, and (iii) better fitness for bacterial adaptation to specific host niches during infection.

Siderophores, hemophores, and citrate are common ferric iron chelators used by bacteria to capture extracellular ferric iron in iron-depleted conditions. The specificity between TBDT and the ferric complex is strict; thus, a TBDT with a broad spectrum for different ferric complexes is less mentioned. The involvement of *fciTABC* in ferric citrate acquisition was reported in our recent study

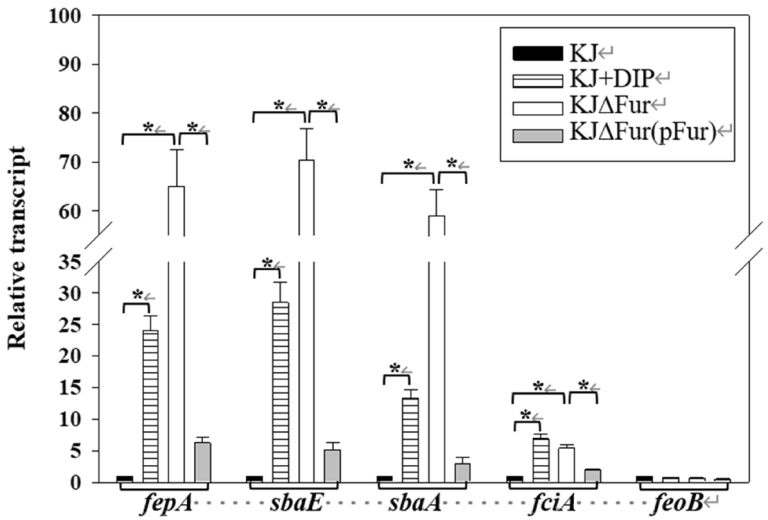

Fig. 4 Impact of iron availability and Fur on the expression of *fepA*, *fciA*, *sbaA*, *sbaE*, and *feoB*. Overnight cultures of *S. maltophilia* KJ, KJΔFur, and KJΔFur(pFur) were inoculated into fresh LB broth at an initial OD_{450nm} of 0.15. KJ cells were prepared as two experimental groups, with or without the treatment of 30 μg/mL DIP. The *fepA*, *fciA*, *sbaA*, *sbaE*, and *feoB* transcripts were quantified by qRT-PCR after a 15-h incubation. The relative transcript level was calculated using the transcript level of KJ cells without DIP treatment as 1. Data is the means from three independent experiments. Bars represent the average values from three independent experiments. Error bars represent the standard deviation for triplicates. *, $P < 0.001$, significance calculated by Student's *t*-test

[19]. In this study, we further revealed the contribution of FciA to the uptake of ferri-stenobactin. However, the participation of *fciTABC* operon in the acquisition of ferric citrate and ferri-stenobactin is not the same. FciA and FciC contribute to the acquisition of both ferric citrate and ferri-stenobactin. However, FciT and FciB uniquely participated in ferric citrate and ferri-stenobactin acquisition, respectively [19].

Compared with the shuttle role of periplasmic FepB in the enterobactin model, the periplasmic proteins involved in ferri-stenobactin shuttle, including FciB, SbaC, and SbaD, seem to be more complicated. None of the three proteins had significant similarity with FepB. FciB is a SEL1-like repeat family protein that may function as an adaptor protein for the assembly of macromolecular complexes [32]. Thus, the possibility that the three proteins (FciB, SbaC, and SbaD) may be assembled into a complex for the shuttle of ferri-stenobactin cannot be immediately ruled out.

The contribution of the putative periplasmic esterase SbaB and inner membrane FeoB to ferri-stenobactin acquisition supported the idea that ferri-stenobactin is hydrolyzed in the periplasm, which is different from the enterobactin model of *E. coli* [9]. This assumption is further supported by the fact that (i) no Fes homolog was found in *S. maltophilia* genome, and (ii) SipA, a homolog of *E. coli* YqjH, is not involved in ferri-stenobactin utilization (Fig. 3). Hisatomi et al. demonstrated that *S. maltophilia* can produce 2,3-dihydroxybenzoylserine (DHBS) as a monomeric unit of stenobactin; however, the exact structure of stenobactin (DHBS complex) has not been elucidated [33]. In addition, Nas and Cianciotto found that FepAsm in *S. maltophilia* cannot uptake *E. coli* enterobactin [22]. These findings strongly suggest that stenobactin and enterobactin share the same DHBS monomer but have distinct structures in the DHBS complex. If this is true, this may explain why no significant protein similarity was observed between *E. coli* Fes and *S. maltophilia* SbaB.

The involvement of periplasmic esterases in ferri-enterobactin hydrolysis has been demonstrated in the IroE of *Salmonella* [34], PfeE of *P. aeruginosa* [35], and Cee of *Campylobacter* [36]. Sequence analysis indicated that SbaB displayed homology to the IroE of *Salmonella* (35% identity and 50% similarity), Cee of *Campylobacter jejuni* (28% identity and 44% similarity), and PfeE of *P. aeruginosa*

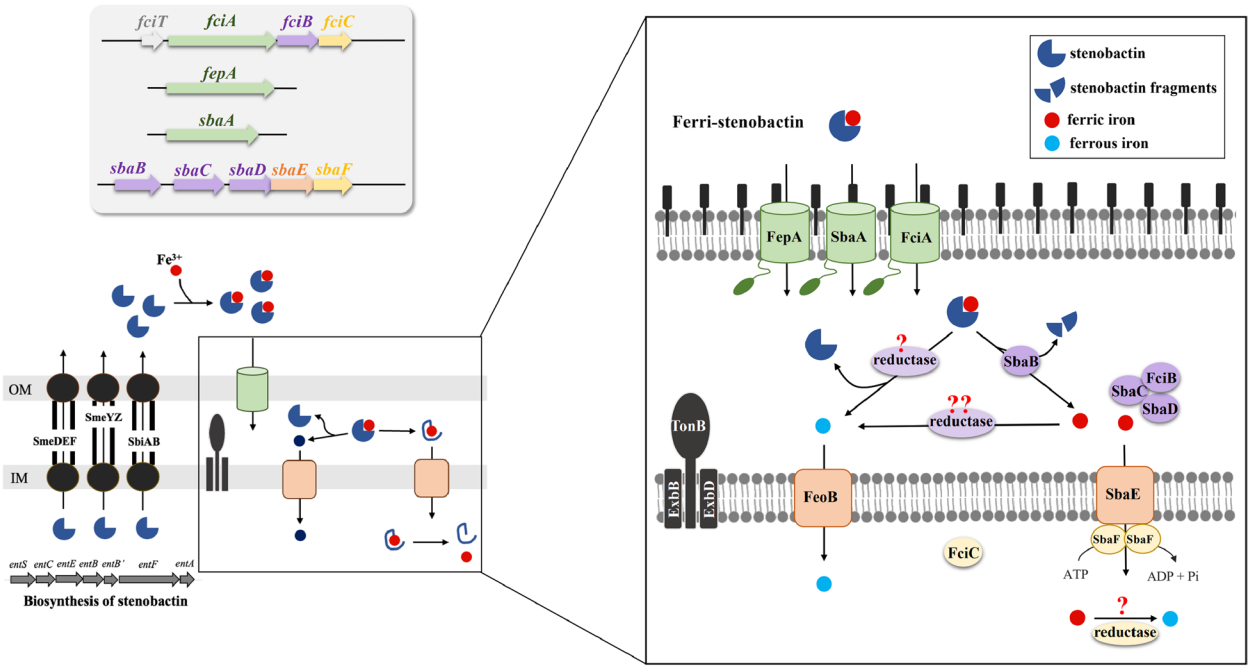

Fig. 5 Stenobactin-mediated iron acquisition system in *S. maltophilia* KJ In an iron-depleted condition, stenobactins, the sole siderophore in *S. maltophilia* KJ, are synthesized by the proteins encoded by *entCEBB'FA* gene cluster and exported into extracellular environment via three efflux pumps SmeDEF, SmeYZ, and SbiAB. Stenobactin binds with ferric iron, and then the ferri-stenobactin complex is uptaken into periplasm via three TBDTs, FepA, FciA, and SbaA. There are two possible routes for the further processing of periplasmic ferri-stenobactin. First, ferri-stenobactin is hydrolyzed by SbaB, and ferric iron is released. Ferric irons are transported into cytoplasm via inner membrane transporter SbaE. SbaC, SbaD, and FciB may assemble as a complex, assisting in this transportation. The ferric iron is further reduced into ferrous iron in cytoplasm. Second, the released ferric iron is reduced into ferrous iron by an unidentified periplasmic reductase. Then, the ferrous iron is transported into cytoplasm via FeoB

(40% identity and 52% similarity). The structure of PfeE was resolved, and the involvement of the GXSXXG motif (residues 155–160), E217, and H258 residues in the catalytic triad was proposed. Alignment of IroE, Cee, PfeE, and SbaB showed that GHSXGG, E217, and H258 are highly conserved among these proteins (Fig. S1), further supporting the possibility that SbaB is an esterase.

If ferri-enterobactin is hydrolyzed in the periplasm, two possibilities should be considered for subsequent iron transportation. First, the released ferric iron is directly reduced to ferrous iron, which is then transported to the cytoplasm via the inner membrane FeoB transporter. Second, the released ferric iron is directly shuttled by periplasmic proteins to a non-FeoB inner membrane transporter and transported into the cytoplasm. Inactivation of *feoB* hardly affected Cee- and PfeE-mediated ferri-enterobactin utilization in *C. jejuni* and *P. aeruginosa*, respectively [35, 36], indicating that the ferric iron model is the favorable one for Cee- and PfeE-mediated inner membrane transportation. However, the *feoB* and *sbaE* mutants of *S. maltophilia* exhibited compromised viability in DIP- and $FeCl_3$-supplemented media (Fig. 3), suggesting that FeoB and SbaE function as the ferrous iron and ferric iron inner membrane transporters, respectively, in *S. maltophilia* KJ. The fact that *feoB* and *sbaE* double mutant (KJΔFeoBΔSbaE) lost the ability to utilize ferri-stenobactin in iron-depleted conditions further supports this assumption.

Conclusion

To integrate the findings of this study with known stenobactin synthesis/secretion systems [19, 24], we portraited a ferri-stenobactin acquisition model in *S. maltophilia* KJ (Fig. 5). Stenobactin, a catecholate-type siderophore, is synthesized in the cytoplasm by proteins encoded by *entCEBB'FA* gene cluster [19] and then secreted into the extracellular environment via the SmeYZ, SmeDEF, and SbiAB pumps [24]. Stenobactin is loaded with ferric iron, and the ferri-stenobactin is subsequently transported into the periplasm by three TBDTs, FepAsm, FciA, and SbaA. Ferri-stenobactin is hydrolyzed by the putative periplasmic esterase SbaB, releasing ferric iron. Some ferric irons are immediately reduced to ferrous iron by an unidentified periplasmic reductase and then transported into the cytoplasm via FeoB. The other ferric irons are directly transported into the cytoplasm via SbaE. In this process, SbaC, SbaD, and FciB may assemble into a complex to facilitate transportation. Subsequently, ferric iron is reduced to ferrous iron by an uncharacterized cytoplasmic reductase.

Abbreviations

DIP	2,2'-Dipyridyl
DHBS	2,3-Dihydroxybenzoylserine
Fur	Ferric uptake regulator
NRPSs	Non-ribosomal peptide synthetase
qRT-PCR	Quantitative real-time PCR
TBDT	TonB-dependent transporter
TPM	Transcripts per kilobase million

Supplementary Information

The online version contains supplementary material available at https://doi.org/10.1186/s12866-025-03792-0.

Supplementary Material 1.

Acknowledgements

Not applicable.

Authors' contributions

TYY prepared Figs. 1–3 HFL prepared Figs. 1 & 5 LHL prpared Figs. 1, 3–4 YTL prpared Figs. 1–2 & 4 TCY prepared Figs. 1–5. All authors reviewed the manuscript.

Funding

This study was funded by the National Science and Technology Council of Taiwan (grant numbers MOST 111–2320-B-A49-025-MY3, NSTC 112–2320-B-A49-043-MY3, and NSTC 112–2320-B-075–005), the Taipei Veterans General Hospital (grant number V113C-225), and the Professor Tsuei-Chu Mong Merit Scholarship (grant number 312260001).

Data availability

All data generated or analyzed during this study are included in this published article and its supplementary information files.

Declarations

Ethics approval and consent to participate

Not applicable.

Consent for publication

Not applicable.

Competing interests

The authors declare no competing interests.

Author details

[1]Present Address: Department of Biotechnology and Laboratory Science in Medicine, National Yang Ming Chiao Tung University, Taipei, Taiwan, Republic of China. [2]Present Address: Department of Medical Laboratory Science and Biotechnology, Asia University, Taichung, Taiwan, Republic of China. [3]Department of Pathology and Laboratory Medicine, Taipei Veterans General Hospital, Taipei, Taiwan, Republic of China. [4]School of Medical Laboratory Science and Biotechnology, College of Medical Science and Technology, Taipei Medical University, Taipei, Taiwan, Republic of China. [5]Division of Infectious Diseases, Department of Medicine, Taipei Veterans General Hospital, Taipei, Taiwan, Republic of China. [6]School of Medicine, National Yang Ming Chiao Tung University, Taipei, Taiwan, Republic of China.

Received: 15 October 2024 Accepted: 29 January 2025
Published online: 25 February 2025

References

1. Schaible UE, Kaufmann SH. Iron and microbial infection. Nat Rev Microbiol. 2004;2(12):946–53.
2. Wandersman C, Delepelaire P. Bacterial iron sources: from siderophores to hemophores. Annu Rev Microbiol. 2004;58:611–47.
3. Paul A, Dubey R. Characterization of protein involved in nitrogen fixation and estimation of CO factor. Appl J Curr Res Biosci Plant Biol. 2015;2:89–97.

4. Raymond KN, Dertz EA, Kim SS. Enterobactin: an archetype for microbial iron transport. Proc Natl Acad Sci U S A. 2003;100(7):3584–8.
5. Köster W. ABC transporter-mediated uptake of iron, siderophores, heme and vitamin B12. Res Microbiol. 2001;152(3–4):291–301.
6. Miethke M, Marahiel MA. Siderophore-based iron acquisition and pathogen control. Microbiol Mol Biol Rev. 2007;71(3):413–51.
7. Horiyama T, Nishino K. AcrB, AcrD, and MdtABC multidrug efflux systems are involved in enterobactin export in *Escherichia coli*. PLoS ONE. 2014;9(9):e108642.
8. Hantke K. Regulation of ferric iron transport in *Escherichia coli* K12: isolation of a constitutive mutant. Mol Gen Genet. 1981;182(2):288–92.
9. Brickman TJ, McIntosh MA. Overexpression and purification of ferric enterobactin esterase from *Escherichia coli.* Demonstration of enzymatic hydrolysis of enterobactin and its iron complex. J Biol Chem. 1992;267(17):12350–5.
10. Miethke M, Hou J, Marahiel MA. The siderophore-interacting protein YqjH acts as a ferric reductase in different iron assimilation pathways of *Escherichia coli*. Biochemistry. 2011;50(50):10951–64.
11. Litwin CM, Calderwood SB. Role of iron in regulation of virulence genes. Clin Microbiol Rev. 1993;6(2):137–49.
12. Miyamoto K, Kosakai K, Ikebayashi S, Tsuchiya T, Yamamoto S, Tsujibo H. Proteomic analysis of *Vibrio vulnificus* M2799 grown under iron-repleted and iron-depleted conditions. Microb Pathog. 2009;46(3):171–7.
13. Escolar L, Pérez-Martín J, de Lorenzo V. Opening the iron box: transcriptional metalloregulation by the Fur protein. J Bacteriol. 1999;181(20):6223–9.
14. Brooke JS. *Stenotrophomonas maltophilia*: an emerging global opportunistic pathogen. Clin Microbiol Rev. 2012;25(1):2–41.
15. Gil-Gil T, Martínez JL, Blanco P. Mechanisms of antimicrobial resistance in *Stenotrophomonas maltophilia*: a review of current knowledge. Expert Rev Anti Infect Ther. 2020;18(4):335–47.
16. Klebba PE, Newton SMC, Six DA, Kumar A, Yang T, Nairn BL, et al. Iron Acquisition Systems of Gram-negative bacterial pathogens define TonB-dependent pathways to novel antibiotics. Chem Rev. 2021;121(9):5193–239.
17. Kalidasan V, Azman A, Joseph N, Kumar S, Awang Hamat R, Neela VK. Putative iron acquisition systems in *Stenotrophomonas maltophilia*. Molecules. 2018;23(8):2048.
18. Pan SY, Shih YL, Huang HH, Li LH, Lin YT, Yang TC. The involvement of PaclRA system of *Stenotrophomonas maltophilia* in the uptake of *Pseudomonas aeruginosa* pyochelin and intraspecies competition for iron acquisition. J Microbiol Immunol Infect. 2022;55(2):273–81.
19. Liao CH, Lu HF, Huang HH, Chen Y, Li LH, Lin YT, et al. The *fciTABC* and *feoABI* systems contribute to ferric citrate acquisition in *Stenotrophomonas maltophilia*. J Biomed Sci. 2022;29(1):26.
20. Shih YL, Wu CM, Lu HF, Li LH, Lin YT, Yang TC. Involvement of the *hemP-hemA-smlt0796-smlt0797* operon in hemin acquisition by *Stenotrophomonas maltophilia*. Microbiol Spectr. 2022;10(3): e0032122.
21. Liao CH, Lu HF, Yang CW, Yeh TY, Lin YT, Yang TC. HemU and TonB1 contribute to hemin acquisition in *Stenotrophomonas maltophilia*. Front Cell Infect Microbiol. 2024;14:1380976.
22. Nas MY, Cianciotto NP. *Stenotrophomonas maltophilia* produces an EntC-dependent catecholate siderophore that is distinct from enterobactin. Microbiology (Reading). 2017;163(11):1590–603.
23. Liao CH, Chen WC, Li LH, Lin YT, Pan SY, Yang TC. AmpR of *Stenotrophomonas maltophilia* is involved in stenobactin synthesis and enhanced β-lactam resistance in an iron-depleted condition. J Antimicrob Chemother. 2020;75(12):3544–51.
24. Wu CJ, Chen Y, Li LH, Wu CM, Lin YT, Ma CH, et al. Roles of SmeYZ, SbiAB, and SmeDEF efflux systems in iron homeostasis of *Stenotrophomonas maltophilia*. Microbiol Spectr. 2022;10(3): e0244821.
25. Fleming TP, Nahlik MS, Neilands JB, McIntosh MA. Physical and genetic characterization of cloned enterobactin genomic sequences from *Escherichia coli* K-12. Gene. 1985;34(1):47–54.
26. Huang YW, Huang HH, Huang KH, Chen WC, Lin YT, Hsu CC, et al. AmpI functions as an iron exporter to alleviate β-lactam-mediated reactive oxygen species stress in *Stenotrophomonas maltophilia*. Antimicrob Agents Chemother. 2019;63(4):e02467–18.
27. Livak KJ, Schmittgen TD. Analysis of relative gene expression data using real-time quantitative PCR and the 2(-Delta Delta C(T)) Method. Methods. 2001;25(4):402–8.
28. Wu CM, Li LH, Lin YL, Wu CJ, Lin YT, Yang TC. The *sbiTRS* operon contributes to stenobactin-mediated iron utilization in *Stenotrophomonas maltophilia*. Microbiol Spectr. 2022;10(6): e0267322.
29. Andrews SC, Robinson AK, Rodríguez-Quiñones F. Bacterial iron homeostasis. FEMS Microbiol Rev. 2003;27(2–3):215–37.
30. Crossman LC, Gould VC, Dow JM, Vernikos GS, Okazaki A, Sebaihia M, et al. The complete genome, comparative and functional analysis of *Stenotrophomonas maltophilia* reveals an organism heavily shielded by drug resistance determinants. Genome Biol. 2008;9(4):R74.
31. Frick-Cheng AE, Sintsova A, Smith SN, Pirani A, Snitkin ES, Mobley HLT. Ferric citrate uptake is a virulence factor in uropathogenic *Escherichia coli*. mBio. 2022;13(3):e0103522.
32. Mittl PR, Schneider-Brachert W. Sel1-like repeat proteins in signal transduction. Cell Signal. 2007;19(1):20–31.
33. Hisatomi A, Shiwa Y, Fujita N, Koshino H, Tanaka N. Identification and structural characterisation of a catecholate-type siderophore produced by *Stenotrophomonas maltophilia* K279a. Microbiology (Reading). 2021; 167(7).
34. Zhu M, Valdebenito M, Winkelmann G, Hantke K. Functions of the siderophore esterases IroD and IroE in iron-salmochelin utilization. Microbiology (Reading). 2005;151(Pt 7):2363–72.
35. Perraud Q, Moynié L, Gasser V, Munier M, Godet J, Hoegy F, et al. A key role for the periplasmic PfeE esterase in iron acquisition via the siderophore enterobactin in *Pseudomonas aeruginosa*. ACS Chem Biol. 2018;13(9):2603–14.
36. Zeng X, Mo Y, Xu F, Lin J. Identification and characterization of a periplasmic trilactone esterase, Cee, revealed unique features of ferric enterobactin acquisition in Campylobacter. Mol Microbiol. 2013;87(3):594–608.

Publisher's Note